Steel and Composite Structures, *Vol. 17, No. 4 (2014) 535-548*
DOI: http://dx.doi.org/10.12989/scs.2014.17.4.535

Torsional analysis of heterogeneous magnetic circular cylinder

Ashraf M. Zenkour *[1,2]

[1] *Department of Mathematics, Faculty of Science, King Abdulaziz University, Jeddah 21589, Saudi Arabia*
[2] *Department of Mathematics, Faculty of Science, Kafrelsheikh University, Kafr El-Sheikh 33516, Egypt*

(*Received December 26, 2013, Revised March 24, 2014, Accepted March 28, 2014*)

Abstract. In this paper, the exact closed-form solutions for torsional analysis of heterogeneous magnetostrictive circular cylinder are derived. The cylinder is subjected to the action of a magnetic field produced by a constant longitudinal current density. It is also acted upon by a particular kind of shearing stress at its upper base. The rigidity of the cylinder is graded through its axial direction from one material at the lower base to another material at the upper base. The distributions of circumferential displacement and shear stresses are presented through the radial and axial directions of the cylinder. The influence of the magnetostrictive parameter is discussed. The effects of additional parameters are investigated.

Keywords: circular cylinder; torsion; magnetostrictive; heterogeneous

1. Introduction

Magnetostrictive materials develop many mechanical deformations when subjected to magnetic fields. This phenomenon is due to rotation of small magnetic fields in the material, which are randomly oriented when the material is not exposed to a magnetic field. Orientation of this small area of the imposition of the magnetic field creates a strain field. As the intensity of the magnetic field is increased, more magnetic domains orientate themselves so that their principal axes of anisotropy are collinear with the magnetic field in each region and finally saturation is achieved.

Magnetostrictive materials have been used as members in functionally graded materials (FGM) for mechanical engineering applications (Wojciechowski 2000). Multilayered composites consisting of piezoelectric and magnetostrictive layers are predicted to have important applications in various devices (Ryu *et al*. 2002) and show a strong magnetoelectric effect which is not present in the individual phases (Wan *et al*. 2003). Different methods are used to study the transient responses of laminated magnetostrictive plates under thermal vibration. The analytical solutions for FGM shells of embedded magnetostrictive layers under vibration are derived (Pradhan 2005). The generalized differential quadrature (GDQ) method is used to study the laminated magneto-strictive plates under thermal vibrations (Hong 2007, 2009, 2010). The transient responses of multilayered magneto-electro-elastic hollow sphere composed of piezoelectric and magnetostrictive layers are investigated (Wang and Ding 2007). The dynamic behavior of a multilayered, perfectly bonded piezoelectric-magnetostrictive composite hollow cylinder under

*Corresponding author, Professor, E-mail: zenkour@kau.edu.sa

http://www.techno-press.org/?journal=scs&subpage=8 ISSN: 1229-9367 (Print), 1598-6233 (Online)

radial deformation is investigated (Wang *et al*. 2009). A dynamic solution for the propagation of harmonic waves inhomogeneous magneto-electro-elastic plates composed of piezoelectric and magnetostrictive materials is presented (Wu *et al*. 2008).

The torsional surface wave propagation in elastic and viscoelastic cylinders is available in the literature. Singh and Yadava (1971) have dealt with the torsional oscillation in a viscoelastic hollow cylinder in magnetic field. Arain and Ahiri (1981) have investigated the magneto-elastic torsional waves in a composite inhomogeneous cylindrical shell under initial stress. Tarn and Chang (2005) have presented the thermoelectroelastic analysis of piezoelectric circular cylinders under extension, torsion, bending, pressuring, shearing, and temperature changes. Taliercio (2010) has solved the torsion problem for hollow circular elastic cylinders analytically. Kakar (2014) has investigated the torsional wave propagation in inhomogeneous viscoelastic cylindrically aeolotropic material permeated by an electro-magneto field.

Many investigations have been done for inhomogeneous media. Among them, for purely elastic cylinders, the special case that the material properties vary as a power law dependence on the radial or axial coordinate has been studied (Zenkour 2006a, b, 2011, 2012). The present work is a predictive assessment of the shearing stresses in and a circumferential displacement of a heterogeneous magnetostrictive circular cylinder. A unified governing equation will be first derived from the basic equilibrium equations taking into account the inclusion of the magnetic intensity. Applying the mixed boundary and curved surface conditions to obtain the analytical solution according to three familiar cases. A number of numerical examples are given and the effect of different parameters is discussed.

2. Basic equations

Let us consider a magnetostrictive, heterogeneous cylinder of radius b and of length l subjected to a torsional deformation due to a shearing force at its end $z = 0$. The cylindrical polar coordinates (r, θ, z) are used as coordinates of reference with positive direction on the z-axis along the axis of the cylinder as shown in Fig. 1. The present cylinder is subjected to the action of a circumferential magnetic field produced by an axial current of constant density J_0.

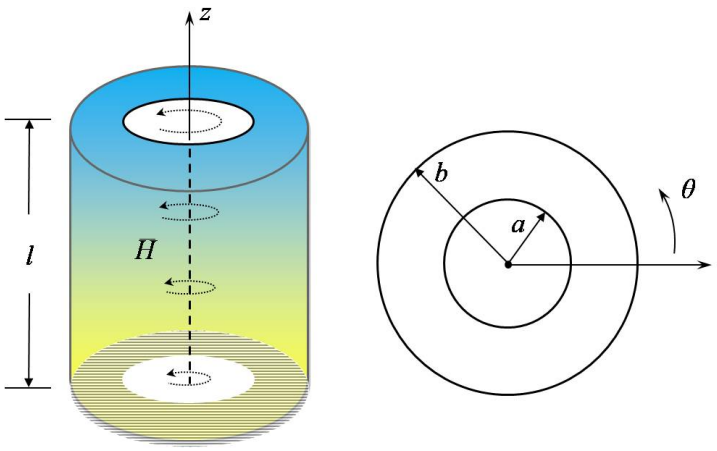

Fig. 1 The geometry and coordinates of a typical heterogeneous circular cylinder

Stress-strain relations may be reduced to express the shear stresses $\sigma_{\theta z}$ and $\sigma_{r\theta}$ in terms of their strains $\varepsilon_{\theta z}$, $\varepsilon_{r\theta}$ and the magnetic field $\overline{H} \equiv (H_r, H_\theta, H_z)$ as (Mukhopadhyay 1980)

$$\begin{aligned} \sigma_{\theta z} &= G(z)\varepsilon_{\theta z} + qH_\theta H_z, \\ \sigma_{r\theta} &= G(z)\varepsilon_{r\theta} + qH_r H_\theta, \end{aligned} \tag{1}$$

where q is the usual magnetostrictive constant and $G(z)$ is the modulus of rigidity.

It is assumed that the cross-section of the layer is not rotated and the displacements in the radial and axial directions are vanished, that is

$$u_r = 0, \quad u_\theta = v(r,z), \quad u_z = 0. \tag{2}$$

Then, the strains $\varepsilon_{\theta z}$ and $\varepsilon_{r\theta}$ may be given by

$$\varepsilon_{\theta z} = \frac{\partial v}{\partial z}, \quad \varepsilon_{r\theta} = \frac{\partial v}{\partial r} - \frac{v}{r}. \tag{3}$$

In addition, the magnetic intensity field is given by

$$\overline{H} \equiv (0, J_0.r, H_0). \tag{4}$$

The equations of equilibrium $\sigma_{ij,j} = 0$, with neglecting the body forces may be reduced to

$$\frac{\partial \sigma_{r\theta}}{\partial r} + \frac{\partial \sigma_{\theta z}}{\partial z} + \frac{2}{r}\sigma_{r\theta} = 0. \tag{5}$$

Substituting Eqs. (1), (3) and (4) into Eq. (5), yields

$$G(z)\left(\frac{\partial^2 v}{\partial r^2} + \frac{1}{r}\frac{\partial v}{\partial r} - \frac{v}{r^2} + \frac{\partial^2 v}{\partial z^2}\right) + \frac{dG}{dz}\frac{\partial v}{\partial z} = 0. \tag{6}$$

The modulus of rigidity $G(z)$ is given by

$$G(z) = G_1 e^{nz/l}, \quad n = \ln\left(\frac{G_2}{G_1}\right), \tag{7}$$

where G_1 is the shear modulus of the first material at lower base and G_2 is the shear modulus of the second material at upper base. Therefore, Eq. (6) tends to

$$\frac{\partial^2 v}{\partial r^2} + \frac{1}{r}\frac{\partial v}{\partial r} - \frac{v}{r^2} + \frac{\partial^2 v}{\partial z^2} + \frac{n}{l}\frac{\partial v}{\partial z} = 0. \tag{8}$$

The mixed boundary conditions for the present problem are given by

$$v|_{z=l} = 0, \quad \sigma_{\theta z}|_{z=0} = f(r), \quad f(r) = \begin{cases} 0, & 0 \le r \le a \\ \Omega r, & a \le r \le b \end{cases} \tag{9}$$

where Ω is the angular displacement of the cylinder. The curved surface $r = b$ of the cylinder is free from mechanical reactions, that is

$$\sigma_{r\theta}|_{r=b} = 0. \tag{10}$$

3. Solution of the problem

A solution of a linear partial differential equation, Eq. (8), is a function $v(r, z)$ of two independent variables that possesses all partial derivatives occurring in the equation and that satisfies the equation in some region of the rz-plane.

Substituting $v(r, z) = u(r)w(z)$ into the partial differential equation, Eq. (8), yields

$$\left[\frac{d^2u}{dr^2} + \frac{1}{r}\frac{du}{dr} - \frac{u^2}{r}\right]\frac{1}{u} = -\left[\frac{d^2w}{dz^2} + \frac{n}{l}\frac{dw}{dz}\right]\frac{1}{w}. \tag{11}$$

Since the left-hand side of the last equation is independent of z and is equal to the right-hand side, which is independent of r, we conclude that each side of the equation must be a constant. As a practical matter it is convenient to write this real separation constant as $-\mu$. From the two equalities we obtain the two linear ordinary differential equations

$$\frac{d^2u}{dr^2} + \frac{1}{r}\frac{du}{dr} + \left(\mu - \frac{1}{r^2}\right)u = 0, \quad \frac{d^2w}{dz^2} + \frac{n}{l}\frac{dw}{dz} - \mu w = 0. \tag{12}$$

We have three cases for μ: zero, positive, or negative; that is, $\mu = 0$, $\mu = \lambda^2 > 0$, and $\mu = -\lambda^2 < 0$, where $\lambda > 0$.

3.1 Case I ($\mu = 0$)

The differential equations in Eq. (12) can be solved by integration. The solutions are $u = c_{11}r + c_{12}/r$ and $w = c_{13} + c_{14}e^{-nz/l}$. However, $u(r)$ is divergent at $r = 0$. The associated coefficient c_{12} is forced to be zero to obtain a physically meaningful result when there is no source or sink at $r = 0$. Thus a particular product solution for the given PDE, Eq. (8) is

$$v = Ar + Bre^{-nz/l}, \tag{13}$$

where $c_{11}c_{13}$ and $c_{11}c_{14}$ are replaced by A and B, respectively. The corresponding stresses are expressed as

$$\begin{aligned} \sigma_{\theta z} &= -\frac{nG_1}{l}Br + qrJ_0H_0, \\ \sigma_{r\theta} &= 0. \end{aligned} \tag{14}$$

The second boundary condition presented in Eq. (9) should be integrated between the limits $r = 0$ and $r = b$. So, both mixed boundary conditions give

$$A = -Be^{-n}, \quad B = \frac{l}{nG_1}\left[qJ_0H_0 - \Omega\left(1 - \frac{a^2}{b^2}\right)\right]. \tag{15}$$

Therefore, the circumferential displacement v and the shear stress $\sigma_{\theta z}$ can be determined easily for this case. From Eqs. (13)-(15), one gets

$$v=\frac{lr}{nG_1}\left[qJ_0H_0-\Omega\left(1-\frac{a^2}{b^2}\right)\right]\left(e^{-nz/l}-e^{-n}\right), \tag{16}$$

$$\sigma_{\theta z}=\Omega r\left(1-\frac{a^2}{b^2}\right). \tag{17}$$

So, the displacement is given in terms of a constant value of the magnetic field. However, the shear stress is independent of the magnetic field.

3.2 Case II ($\mu=\lambda^2$)

The general solutions of Eqs. (12) are

$$\begin{aligned} u&=c_{21}J_1(\lambda r)+c_{22}Y_1(\lambda r),\\ w&=c_{23}e^{n_1z/l}+c_{24}e^{n_2z/l}, \end{aligned} \tag{18}$$

where $J_1(\lambda r)$ and $Y_1(\lambda r)$ are the Bessel functions of the first and second kind, respectively, and n_1, $n_2=-\frac{1}{2}\left(n\pm\sqrt{n^2+4l^2\lambda^2}\right)$. Thus, another particular product solution of Eq. (8) is

$$v=\left[\overline{A}e^{n_1z/l}+\overline{B}e^{n_1z/l}\right]J_1(\lambda r)+\left[\overline{C}e^{n_1z/l}+\overline{D}e^{n_2z/l}\right]Y_1(\lambda r), \tag{19}$$

where $\overline{A}=c_{21}c_{23}$, $\overline{B}=c_{21}c_{24}$, $\overline{C}=c_{22}c_{23}$ and $\overline{D}=c_{22}c_{24}$. However, $Y_1(\lambda r)$ is divergent at $r=0$. The associated coefficient c_{22} is forced to be zero to obtain a physically meaningful result when there is no source or sink at $r=0$. Thus, the circumferential displacement becomes

$$v=\left[\overline{A}e^{n_1z/l}+\overline{B}e^{n_1z/l}\right]J_1(\lambda r). \tag{20}$$

The corresponding stresses are expressed as

$$\begin{aligned} \sigma_{\theta z}&=\frac{G_1}{l}e^{nz/l}\left[\overline{A}n_1e^{n_1z/l}+\overline{B}n_2e^{n_1z/l}\right]J_1(\lambda r)+qJ_0H_0,\\ \sigma_{r\theta}&=-\lambda G_1e^{nz/l}\left[\overline{A}e^{n_1z/l}+\overline{B}e^{n_1z/l}\right]J_2(\lambda r), \end{aligned} \tag{21}$$

in which

$$J_2(\lambda r)=\frac{2}{\lambda r}J_1(\lambda r)-J_0(\lambda r). \tag{22}$$

The surface condition given in Eq. (10) yields

$$J_2(\lambda_k b)=0,\quad k=1,2,3,\ldots. \tag{23}$$

The first mixed condition, given in Eq. (9), gives

$$\overline{A}_k e^{n_1} + \overline{B}_k e^{n_2} = 0. \tag{24}$$

From the second mixed condition given in Eq. (9), one obtains

$$\frac{G_1}{l}\sum_{k=1}^{\infty}\left[\overline{A}_k n_1 + \overline{B}_k n_2\right] J_1(\lambda_k r) + qrJ_0 H_0 = f(r). \tag{25}$$

Multiplying both sides of the above equation by $rJ_1(\lambda_k r)$ and integrating between the limits $r = 0$ and $r = b$, we get

$$\frac{G_1}{l}\left[\overline{A}_k n_1 + \overline{B}_k n_2\right]\int_0^b rJ_1^2(\lambda_k r)dr = \Omega\int_a^b r^2 J_1(\lambda_k r)dr, \tag{26}$$

or

$$\overline{A}_k n_1 + \overline{B}_k n_2 = \frac{-2l\Omega a^2 J_2(\lambda_k a)}{G_1 b^2 \lambda_k J_1^2(\lambda_k b)}. \tag{27}$$

Solving Eqs. (24) and (27) for $\overline{A}_k$ and $\overline{B}_k$, one get

$$\overline{A}_k = \frac{2l\Omega a^2 e^{n_2} J_2(\lambda_k a)}{(n_2 e^{n_1} - n_1 e^{n_2}) G_1 b^2 \lambda_k J_1^2(\lambda_k b)}, \quad \overline{B}_k = -e^{n_1 - n_2}\overline{A}_k. \tag{28}$$

With the aid of the above equation, one can obtain the final forms of the circumferential displacement and shearing stresses. It is to be noted that, the magnetic field affects the shearing stress $\sigma_{\theta z}$ to the extent of the addition of a term varying linearly with the radial distance.

3.3 Case III ($\mu = -\lambda^2$)

The general solutions of Eq. (12) are

$$\begin{aligned} u &= c_{31} I_1(\lambda r) + c_{32} K_1(\lambda r), \\ w &= c e^{m_1 z/l} + c_{34} e^{m_2 z/l}, \end{aligned} \tag{29}$$

where $I_1(\lambda r)$ and $K_1(\lambda r)$ are the modified Bessel functions of the first and second kind, respectively, and $m_1,\ m_2 = -\frac{1}{2}\left(n \pm \sqrt{n^2 + 4l^2\lambda^2}\right)$. It is clear that the modified Bessel function $K_1(\lambda r)$ is divergent at $r = 0$, so the associated coefficient c_{32} is forced to be zero to obtain a physically meaningful result when there is no source or sink at $r = 0$. Thus, the circumferential displacement becomes

$$v = \left[-\hat{A}e^{m_1 z/l} + \hat{B}e^{m_2 z/l}\right] I_1(\lambda r), \tag{30}$$

where $\hat{A} = c_{31}c_{33}$ and $\hat{B} = c_{31}c_{34}$. The corresponding stresses are expressed as

$$\sigma_{\theta z} = \frac{G_1}{l} e^{nz/l}\left[\hat{A} m_1 e^{m_1 z/l} + \hat{B} m_2 e^{m_2 z/l}\right] I_1(\lambda r) + qrJ_0 H_0,$$
$$\sigma_{r\theta} = \lambda G_1 e^{nz/l}\left[\hat{A} e^{m_1 z/l} + \hat{B} e^{m_2 z/l}\right] I_2(\lambda r), \tag{31}$$

in which

$$I_2(\lambda r) = -\frac{2}{\lambda r} I_1(\lambda r) + I_0(\lambda r). \tag{32}$$

The surface condition given in Eq. (10) yields

$$I_2(\lambda_k b) = 0, \quad k = 1, 2, 3, \ldots. \tag{33}$$

The first mixed condition, given in Eq. (9), gives

$$\hat{A}_k e^{m_1} + \hat{B}_k e^{m_2} = 0, \tag{34}$$

while the second mixed condition gives

$$\frac{G_1}{l} \sum_{k=1}^{\infty} \left[\hat{A}_k m_1 + \hat{B}_k m_2\right] I_1(\lambda r) + qrJ_0 H_0 = f(r). \tag{35}$$

Multiplying both sides of the above equation by $rI_1(\lambda_k r)$ and integrating between the limits $r = 0$ and $r = b$, we get

$$\frac{G_1}{l}\left[\hat{A}_k m_1 + \hat{B}_k m_2\right] \int_0^b r I_1^2(\lambda_k r) dr = \Omega \int_a^b r^2 I_1(\lambda_k r) dr, \tag{36}$$

or

$$\hat{A}_k m_1 + \hat{B}_k m_2 = \frac{-2l\Omega a^2 I_2(\lambda_k a)}{G_1 b^2 \lambda_k I_1^2(\lambda_k b)}. \tag{37}$$

Solving Eqs. (34) and (37) for $\hat{A}_k$ and $\hat{B}_k$, one gets

$$\hat{A}_k = \frac{2l\Omega a^2 e^{m_2} I_2(\lambda_k a)}{(m_2 e^{m_1} - m_1 e^{m_2}) G_1 b^2 \lambda_k I_1^2(\lambda_k b)}, \quad \overline{B}_k = -e^{m_1 - m_2} \hat{A}_k. \tag{38}$$

Similarly, one can obtain the final forms of the circumferential displacement and shear stresses. Once again, the magnetic field affects also the shearing stress $\sigma_{\theta z}$ to the extent of the addition of a term varying linearly with the radial distance.

4. Applications

The complete solution corresponding to all cases studied may be presented here by introducing the following dimensionless forms

$$S=\frac{a}{b},\quad Z=\frac{z}{l},\quad R=\frac{r}{b},\quad L=\frac{l}{b},\quad \overline{\lambda}=\lambda b,\quad \overline{q}=\frac{qJ_0H_0}{\Omega},$$
$$\overline{V}=\frac{G_1}{bl\Omega}v(r,z),\quad \overline{\sigma}_{23}=\frac{1}{b\Omega}\sigma_{\theta z}(r,z),\quad \overline{\sigma}_{12}=\frac{1}{b\Omega}\sigma_{r\theta}(r,z). \tag{39}$$

Then, the final form of the displacement and stresses according to Case I are given by

$$\overline{V}=\frac{1-\overline{q}-S^2}{n}(e^{-n}-e^{-nz})R,\quad \overline{\sigma}_{23}=(1-S^2)R,\quad \overline{\sigma}_{12}=0. \tag{40}$$

Also for Case II one gets

$$\begin{aligned}
\overline{V}&=\frac{2S^2J_2(\overline{\lambda}_k a)}{\overline{\lambda}_k(n_2e^{n_1}-n_1e^{n_2})J_1^2(\overline{\lambda}_k)}(e^{n_1+n_2Z}-e^{n_2+n_1Z})J_1(\overline{\lambda}_k R),\\
\overline{\sigma}_{23}&=\frac{2S^2J_2(\overline{\lambda}_k S)}{\overline{\lambda}_k(n_2e^{n_1}-n_1e^{n_2})J_1^2(\overline{\lambda}_k)}(n_1e^{n_2+n_1Z}-n_2e^{n_1+n_2Z})J_1(\overline{\lambda}_k R)+\overline{q}R,\\
\overline{\sigma}_{12}&=\frac{2LS^2J_2(\overline{\lambda}_k S)}{(n_2e^{n_1}-n_1e^{n_2})J_1^2(\overline{\lambda}_k)}e^{nz}(e^{n_1+n_2Z}-e^{n_2+n_1Z})J_2(\overline{\lambda}_k R).
\end{aligned} \tag{41}$$

Finally, the displacement and stresses according to Case III are given by

$$\begin{aligned}
\overline{V}&=\frac{2S^2I_2(\overline{\lambda}_k S)}{\overline{\lambda}_k(m_2e^{m_1}-m_1e^{m_2})I_1^2(\overline{\lambda}_k)}(e^{m_1+m_2Z}-e^{m_2+m_1Z})I_1(\overline{\lambda}_k R),\\
\overline{\sigma}_{23}&=\frac{2S^2I_2(\overline{\lambda}_k S)}{\overline{\lambda}_k(m_2e^{m_1}-m_1e^{m_2})I_1^2(\overline{\lambda}_k)}(m_2e^{m_1+m_2Z}-m_1e^{m_2+m_1Z})I_1(\overline{\lambda}_k R)+\overline{q}R,\\
\overline{\sigma}_{12}&=\frac{2LS^2I_2(\overline{\lambda}_k S)}{(m_2e^{m_1}-m_1e^{m_2})I_1^2(\overline{\lambda}_k)}e^{nz}(e^{m_2+m_1Z}-e^{m_1+m_2Z})I_2(\overline{\lambda}_k R).
\end{aligned} \tag{42}$$

5. Numerical results

We restrict our attention to the most important problem that presented in Case II. Eq. (23) has an infinite number of roots, the first nonzero positive root, $\lambda = 5.13562230184068/b$, is used here. The inhomogeneity parameter $G = G_2/G_1$ is considered here. Numerical results for the dimensionless displacement and stresses are presented in Figs. 2-11. Different values of the aspect ratio $S = a/b$, the inhomogeneity parameter G, and the length-to-radius ratio $L = l/b$ as well as the magnetostrictive parameter q, are all used in the figures. It is assumed, except otherwise stated, that $S = 0.2$, $L = 3$, and $G = 0.5$.

The dimensionless circumferential displacement $V = 10^3\overline{V}$ and shear stresses $(\sigma_{23},\sigma_{12}) = 100\,(\overline{\sigma}_{23},-\overline{\sigma}_{12})$ are plotted according to the following data

$$J_0 = 20\ \text{Am/m}^2\quad H_0 = 100\ \text{Am/m},\quad \Omega = 10^5.$$

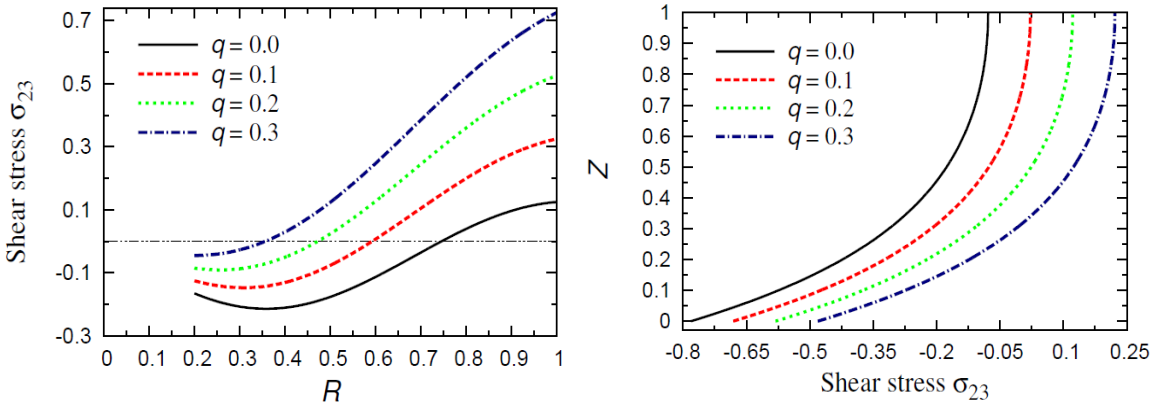

Fig. 2 Effect of the magnetostrictive parameter q on the shear stress σ_{23} along the radial and through the axial directions

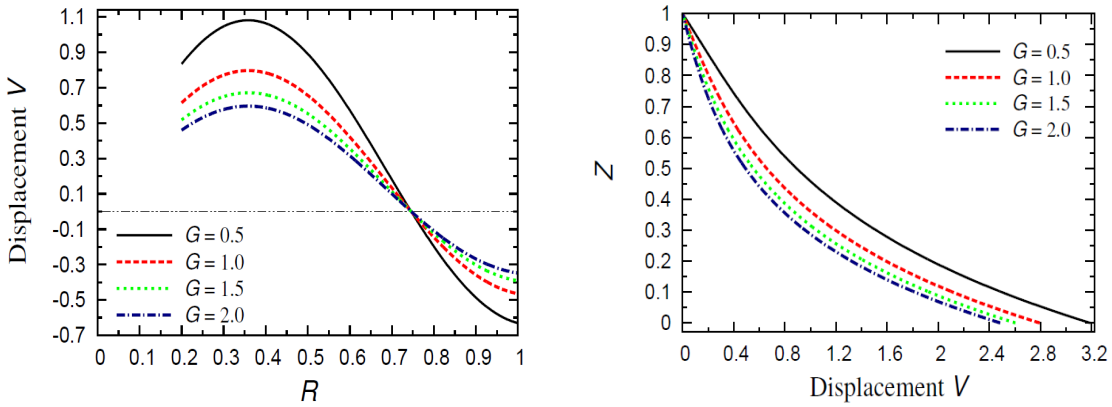

Fig. 3 Effect of the inhomogeneity parameter G on the circumferential displacement V along the radial and through the axial directions

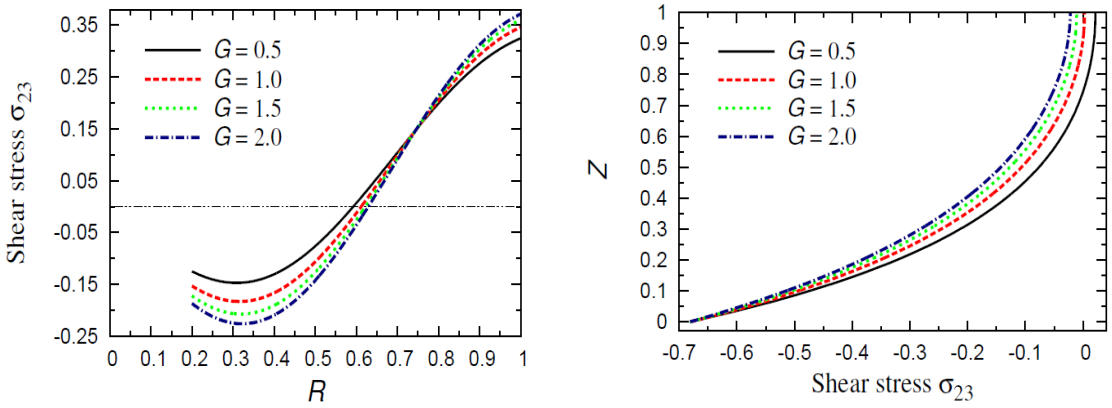

Fig. 4 Effect of the inhomogeneity parameter G on the shear stress σ_{23} along the radial and through the axial directions

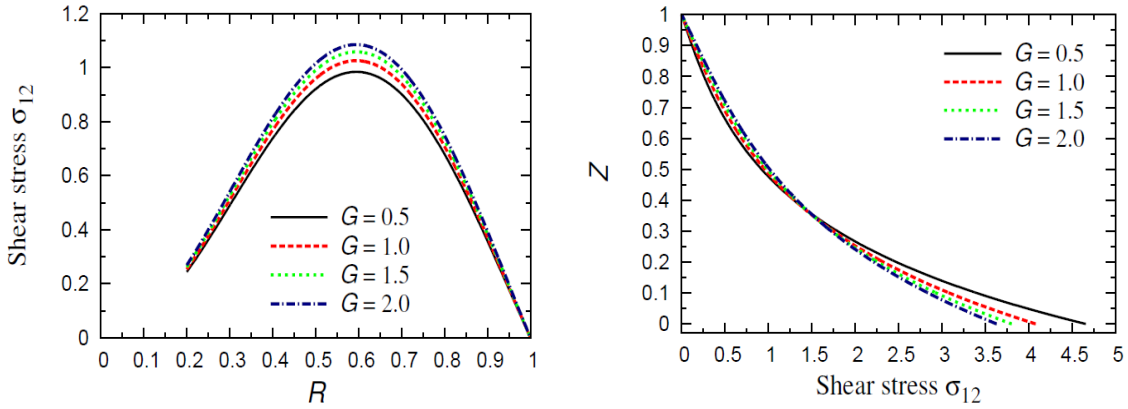

Fig. 5 Effect of the inhomogeneity parameter G on the shear stress σ_{12} along the radial and through the axial directions

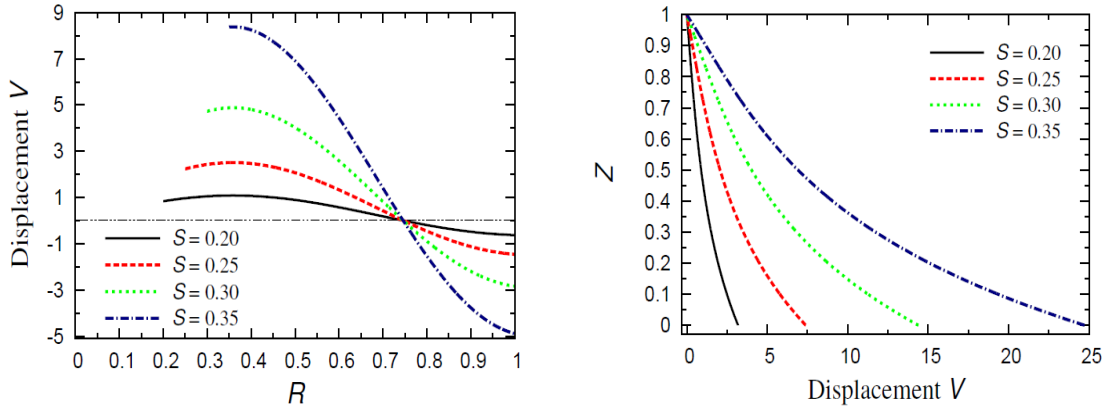

Fig. 6 Effect of the aspect ratio S on the circumferential displacement V along the radial and through the axial directions

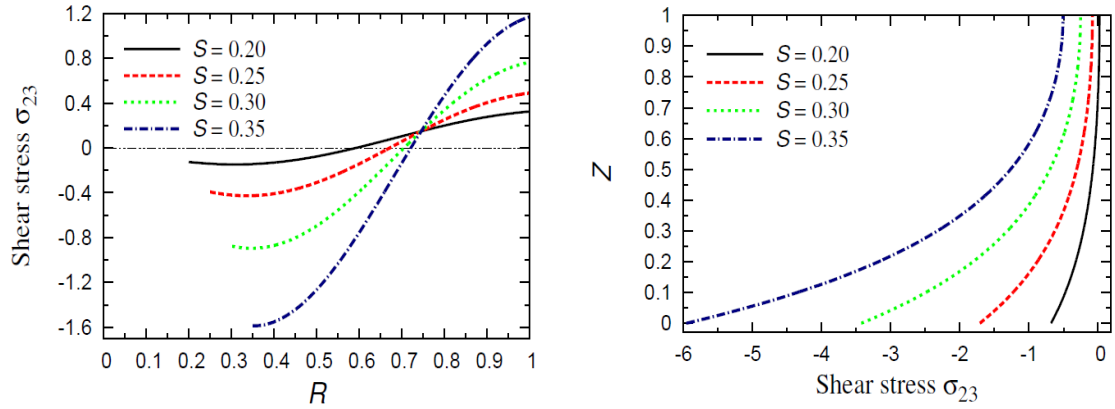

Fig. 7 Effect of the aspect ratio S on the shear stress σ_{23} along the radial and through the axial directions

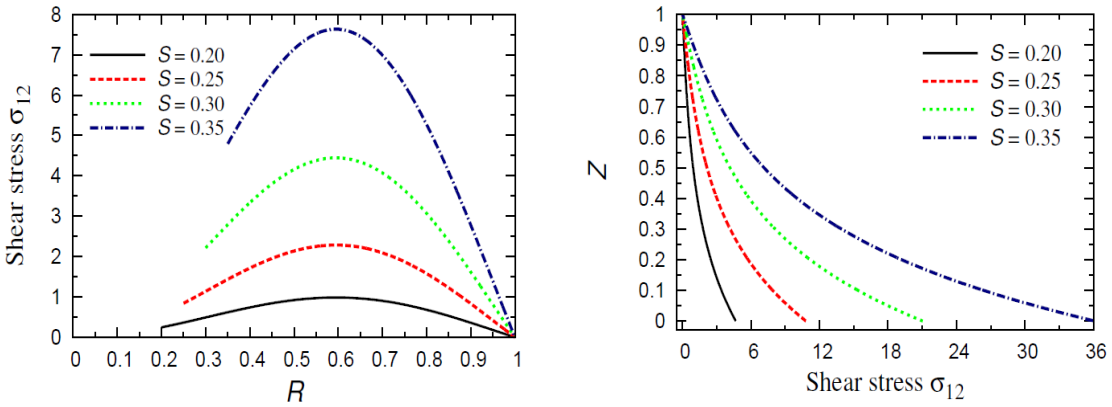

Fig. 8 Effect of the aspect ratio S on the shear stress σ_{12} along the radial and through the axial directions

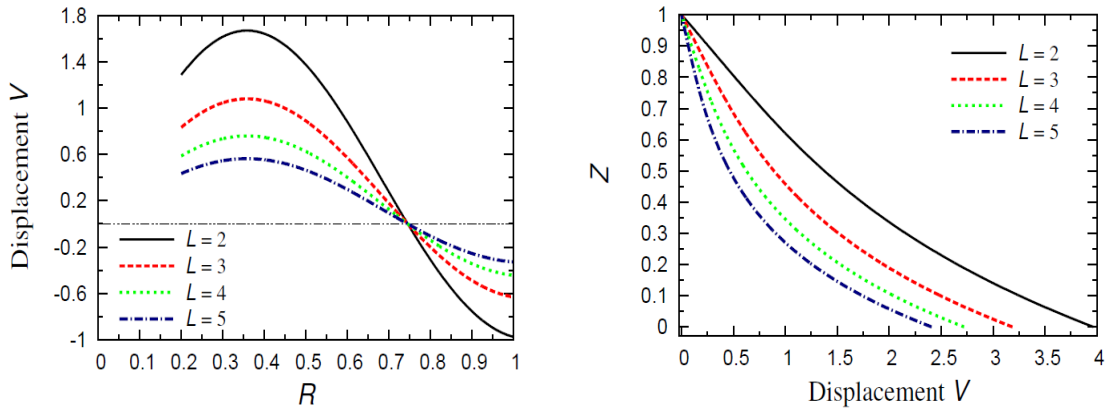

Fig. 9 Effect of the length-to-radius ratio L on the circumferential displacement V along the radial and through the axial directions

Firstly, the effect of the magnetostrictive parameter q on the shear stress σ_{23} is presented in Fig. 2. The shear stress σ_{23} is plotting along the radial and through the axial directions. The little variation of q has highly sensitive on the plots of σ_{23}. The shear stress σ_{23} is increasing as q increases. The stress may be vanish on $0.3 < R < 0.8$ for different values of q. The shear stress σ_{23} is more sensitive to the inclusion of q with the increasing of the radial and axial distances. Also, the shear stress σ_{23} may be changing its direction from negative to positive at some axial positions for magnetostrictive cylinders. However, it is still negative for a non-magnetostrictive cylinder ($q = 0$). In what follows, the value of the magnetostrictive parameter $q = 0.1$ is used for deducing the shear stress σ_{23} only.

The effect of inhomogeneity parameter G is presented in Figs. 3-5. The displacement and stresses are sensitive to the variation of G especially at the inner and outer surfaces of the cylinder. Fig. 3 shows that, as G decreases the absolute value of the displacement is increasing along the radial direction and is decreasing through the axial direction. It is to be noted that the displacement V vanishes at $R \cong 0.746$ and at $Z = 1$ and this irrespective of the value of G. The circumferential displacement V has its maximum absolute value at $R = 0.359$ and at the lower base of the cylinder.

Fig. 4 shows that the absolute value of the shear stress σ_{23} is increasing as G increases. The shear stress vanishes on $0.58 < R < 0.63$ according to the value of G. However, the variation of G has no effect on the shear stress σ_{23} at the position $R \cong 0.746$ in which $\sigma_{23} \cong 0.149$. Also, the shear stress σ_{23} has the same value ($\sigma_{23} = -0.6813$) at the lower base of the cylinder and this irrespective the value of G. Fig. 5 shows that the shear stress σ_{12} increases as G increases for $Z < 0.345$ and vice versa for $Z \geq 0.345$. The maximum value of σ_{12} occurs at $R = 0.595$ on the lower base.

The effect of aspect ratio $S = a/b$ is presented in Figs. 6-8. The displacement and stresses are very sensitive to the variation of S. The absolute values of the displacement and stresses are increasing as S increases. The displacement V vanishes at $R \cong 0.746$ (see Fig. 6(a)) while the variation of S has no effect on the shearing stress σ_{23} at the same position $R \cong 0.746$ in which $\sigma_{23} \cong 0.149$ (see Fig. 7(a)). Fig. 6 shows that the maximum values of V occur at $R = 0.359$ on the lower base of the cylinder. Fig. 7 shows that the shear stress σ_{23} vanishes on $0.58 \leq R \leq 0.72$ according to the value of S. Fig. 8 shows that the shear stress σ_{12} increases as S increases along the radial and through the axial directions, especially at the lower base of the cylinder. The maximum

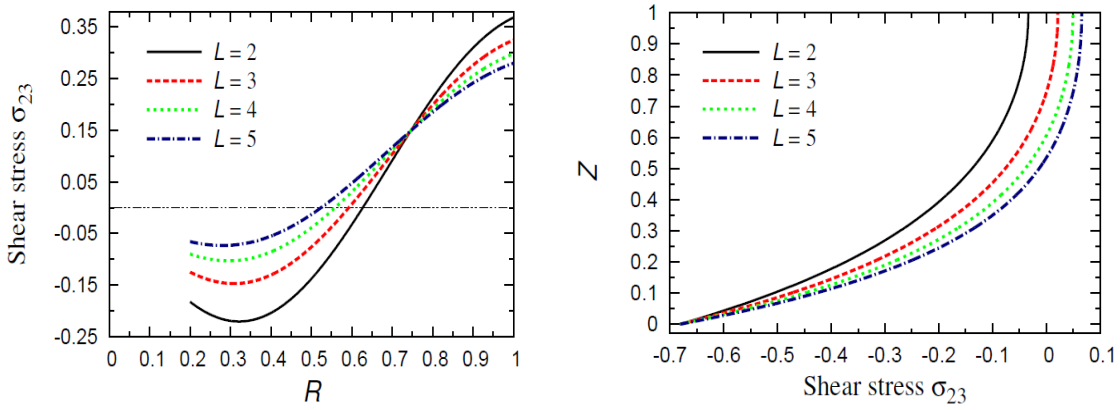

Fig. 10 Effect of the length-to-radius ratio L on the shear stress σ_{23} along the radial and through the axial directions

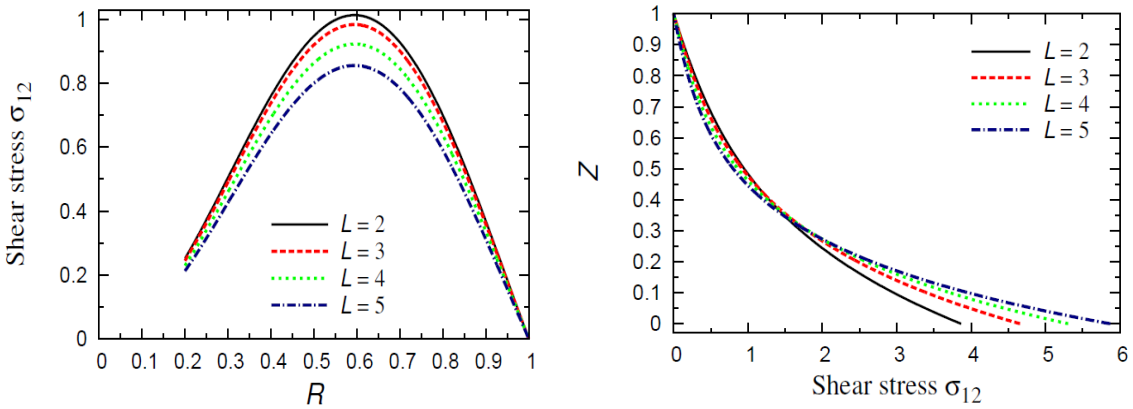

Fig. 11 Effect of the length-to-radius ratio L on the shear stress σ_{12} along the radial and through the axial directions

value of σ_{12} occurs at $R = 0.595$. Generally, the sensitivity of S on the displacement and shear stresses is more pronounced at the lower base of the cylinder.

Finally, the effect of the length-to-radius ratio $L = l/b$ is presented in Figs. 9-11. The displacement and stresses are also sensitive to the variation of L. The absolute values of the displacement and stresses are increasing as L increases along the radial direction. As discussed before, the circumferential displacement V vanishes at $R \cong 0.746$ while the variation of L has no effect on the shearing stress σ_{23} at the same position in which $\sigma_{23} \cong 0.149$. The displacement V has its maximum value at $R = 0.359$ on the upper base of the cylinder. However, the maximum value of σ_{23} is occurred at the upper base ($Z = 1$) and outer surface ($R = 1$) of the cylinder. As L increases, through the axial direction of the cylinder, V is decreasing while σ_{23} is increasing. In addition, the shear stress σ_{12} vanishes only at the outer curved surface of the cylinder ($R = 1$) as well as at the upper base of the cylinder. Once again, Fig. 11 shows that the shear stress σ_{12} decreases as L increases for $Z < 0.345$ and vice versa for $Z \geq 0.345$. The maximum value of σ_{12} occurs at $R = 0.595$ on the lower base.

6. Conclusions

Different analytical solutions of the circumferential displacement and shear stresses are given in terms of the radial and axial co-ordinates of the heterogeneous magnetostrictive circular cylinder. The results are very sensitive to the variation of different parameters such as the aspect ratio, the length-to-radius ratio and the inhomogeneity parameter. Also, the shear stress is very sensitive to the variation of the magnetostrictive parameter. Irrespective of the values of parameters used, the circumferential displacement V vanishes at $R \cong 0.746$ and on the upper base of the cylinder. The maximum absolute value of V is occurred at $R = 0.359$ on the lower base of the cylinder. The maximum value of the shear stress σ_{23} is occurred at the curved surface of the cylinder, especially on the upper base of the cylinder. It has the same value, $\sigma_{23} \cong 0.149$ at $R \cong 0.744$, and this irrespective to the values of the parameters used. However, it has the same value, $\sigma_{23} = -0.6813$ at the lower base of the cylinder for $R = 0.5$, $S = 0.2$, and all values of other parameters. Finally, the maximum value of σ_{12} is occurred at $R \cong 0.595$, especially at the lower base of the heterogeneous magnetostrictive circular cylinder. The exact closed form solutions presented here may be used for future comparison purposes of similar problems of homogeneous ($G = 1$) and/or of non-magnetostrictive material ($q = 0$) cylinders.

References

Arain, S. and Ahiri, L. (1981), "Magneto-elastic torsional waves in a composite non homogeneous cylindrical shell under initial stress", *Def. Sci. J.*, **31**(2), 125-132.

Hong, C.C. (2007), "Thermal vibration of magnetostrictive material in laminated plates by the GDQ method", *Open Mech. J.*, **1**(1), 29-37.

Hong, C.C. (2009), "Transient responses of magnetostrictive plates without shear effects", *Int. J. Eng. Sci.*, **47**(3), 355-362.

Hong, C.C. (2010), "Transient responses of magnetostrictive plates by using the GDQ method", *Eur. J. Mech. A/Solids*, **29**(6), 1015-1021.

Kakar, R. (2014) "Magneto-electro-viscoelastic torsional waves in aeolotropic tube under initial compression stress", *Lat. Am. J. Solids Struct.*, **11**(4), 580-597.

Mukhopadhyay, J. (1980), "A note on torsional deformation of a non-homogeneous magnetostrictive cylinder", *Rev. Roum. Sci. Techn.-Méc. Appl., Tome*, **25**(1), 39-44.
Pradhan, S.C. (2005) "Vibration suppression of FGM shells using embedded magnetostrictive layers", *Int. J. Solid. Struct.*, **42**(9-10), 2465-2488.
Ryu, J., Priya, S., Uchino, K. and Kim, H. (2002), "Magnetoelectric effect in composites of magnetostrictive and piezoelectric materials", *J. Electroceramics*, **8**(2), 107-119.
Singh, P.N. and Yadava, B. (1971), "Torsional oscillation of a viscoelastic cylinder in a magnetic field", *Pure Appl. Geophys.*, **91**(1), 51-55.
Taliercio, A. (2010), "Torsion of micropolar hollow circular cylinders", *Mech. Res. Commun.*, **37**(4), 406-411.
Tarn, J.-Q. and Chang, H.-H. (2005), "Extension, torsion, bending, pressuring, and shearing of piezoelectric circular cylinders with radial inhomogeneity", *J. Intel. Mater. Sys. Struct.*, **16**(7-8), 631-641.
Wang, H.M. and Ding, H.J. (2007), "Radial vibration of piezoelectric/magnetostrictive composite hollow sphere", *J. Sound Vib.*, **307**(1-2), 330-348.
Wang, H.M., Liu, C.B. and Ding, H.J. (2009), "Dynamic behavior of piezoelectric/ magnetostrictive composite hollow cylinder", *Arch. Appl. Mech.*, **79**(8), 753-771.
Wan, J.G., Liu, J.M., Chand, H.L.W., Choy, C.L., Wang, G.H. and Nan, C.W. (2003), "Giant magnetoelectric effect of a hybrid of magnetostrictive and piezoelectric composites", *J. Appl. Phys.*, **93**, 9916-9919.
Wojciechowski, S. (2000), "New trends in the development of mechanical engineering materials", *J. Mater. Proc. Tech.*, **106**(1-3), 230-235.
Wu, B., Yu, J. and He, C. (2008), "Wave propagation in non-homogeneous magneto-electro-elastic plates", *J. Sound Vib.*, **317**(1-2), 250-264.
Zenkour, A.M. (2006a), "Rotating variable-thickness orthotropic cylinder containing a solid core of uniform-thickness", *Arch. Appl. Mech.*, **76**(1-2), 89-102.
Zenkour, A.M. (2006b), "Stresses in cross-ply laminated circular cylinders of axially variable thickness", *Acta Mech.*, **187**(1-4) 85-102.
Zenkour, A.M. (2011), "Stresses in a rotating variable-thickness heterogeneous viscoelastic composite cylinder", *Appl. Math. Mech. - Engl. Ed.*, **32**(4) 1-14.
Zenkour, A.M. (2012), "Dynamical bending analysis of functionally graded infinite cylinder with rigid core", *Appl. Math. Comput.*, **218**(17), 8997-9006.